

# Near-IR Excitation Transfer and Electron Transfer in a BF<sub>2</sub>-Chelated Dipyrromethane–Azadipyrromethane Dyad and Triad

Mohamed E. El-Khouly,<sup>[a]</sup> Anu N. Amin,<sup>[b]</sup> Melvin E. Zandler,<sup>[b]</sup>  
Shunichi Fukuzumi,<sup>\*[a, c]</sup> and Francis D'Souza<sup>\*[b, d]</sup>

**Abstract:** A molecular dyad and triad, comprised of a known photosensitizer, BF<sub>2</sub>-chelated dipyrromethane (BDP), covalently linked to its structural analog and near-IR emitting sensitizer, BF<sub>2</sub>-chelated tetraarylazadipyrromethane (ADP), have been newly synthesized and the photoinduced energy and electron transfer were examined by femtosecond and nanosecond laser flash photolysis. The structural integrity of the newly synthesized compounds has been established by spectroscopic, electrochemical, and computational methods. The DFT calculations revealed a molecular-clip-type structure for the triad, in which the BDP and ADP entities are separated by about 14 Å with a dihedral angle between the fluorophores of around 70°. Differen-

tial pulse voltammetry studies have revealed the redox states, allowing estimation of the energies of the charge-separated states. Such calculations revealed a charge separation from the singlet excited BDP (<sup>1</sup>BDP\*) to ADP (BDP<sup>•+</sup>-ADP<sup>•-</sup>) to be energetically favorable in nonpolar toluene and in polar benzonitrile. In addition, the excitation transfer from the singlet BDP to ADP is also envisioned due to good spectral overlap of the BDP emission and ADP absorption spectra. Femtosecond laser flash photolysis studies provided concrete evidence for the oc-

currence of energy transfer from <sup>1</sup>BDP\* to ADP (in benzonitrile and toluene) and electron transfer from BDP to <sup>1</sup>ADP\* (in benzonitrile, but not in toluene). The kinetic study of energy transfer was measured by monitoring the rise of the ADP emission and revealed fast energy transfer (ca. 10<sup>11</sup> s<sup>-1</sup>) in these molecular systems. The kinetics of electron transfer via <sup>1</sup>ADP\*, measured by monitoring the decay of the singlet ADP at λ = 820 nm, revealed a relatively fast charge-separation process from BDP to <sup>1</sup>ADP\*. These findings suggest the potential of the examined ADP–BDP molecules to be efficient photosynthetic antenna and reaction center models.

**Keywords:** chelates • donor–acceptor systems • electron transfer • energy transfer • near-IR emitters

## Introduction

Molecular and supramolecular systems linked to two or more fluorophores have attracted increased interest from the scientific community due to their potential applications,

which range from solar-energy harvesting and energy conversion to molecular logic gates and optoelectronic devices.<sup>[1–7]</sup> Tetrapyrrole macrocycles, such as porphyrins and phthalocyanines, have widely been used for these applications due to their structural similarity to natural photosynthetic pigments, established synthesis protocols, and tunable redox and photophysical properties.<sup>[8]</sup> Interestingly, another class of fluorophores, BF<sub>2</sub>-chelated dipyrromethanes (BODIPY or BDP),<sup>[9]</sup> have also recently been employed to perform the functionalities of antennas and electron donors or acceptors in a number of molecular systems.<sup>[10–18]</sup> This is because the BDP macrocycle can be easily modified at the *meso* and β-carbon positions and exhibits attractive photophysical characteristics with strong absorption and emission bands in the visible region.<sup>[9,19]</sup>

A structural analog of BDP, BF<sub>2</sub>-chelated tetraarylazadipyrromethanes (Aza-BODIPY or ADP), which have a nitrogen in the *meso* position of the macrocycle, have attracted increased attention because of their high extinction coefficients (7–8 × 10<sup>5</sup> M<sup>-1</sup> cm<sup>-1</sup>), large fluorescence quantum yields above λ = 700 nm, and facile one-electron reduction potentials.<sup>[20]</sup> Thus, they have been used in applications ranging from photosensitizers to photodynamic therapy agents.<sup>[21]</sup> Recently, we reported on donor–acceptor dyads and triads

[a] Dr. M. E. El-Khouly, Prof. S. Fukuzumi  
Department of Material and Life Science  
Graduate School of Engineering, Osaka University  
Suita, Osaka 565-0871 (Japan)  
Fax: (+81)6-6879-7370  
E-mail: fukuzumi@chem.eng.osaka-u.ac.jp

[b] A. N. Amin, Prof. M. E. Zandler, Prof. F. D'Souza  
Department of Chemistry  
Wichita State University, KS 67260-0051 (USA)

[c] Prof. S. Fukuzumi  
Department of Bioinspired Science, Ewha Womans University  
Seoul 120-750 (Korea)

[d] Prof. F. D'Souza  
Department of Chemistry, University of North Texas  
1155 Union Circle, #305070, Denton, TX 76203-5017 (USA)  
E-mail: Francis.DSouza@UNT.edu

Supporting information for this article is available on the WWW under <http://dx.doi.org/10.1002/chem.201103074>, and contains the mass spectra of the new compounds, excitation spectra, and transient absorption spectra of the compounds in toluene and benzonitrile.

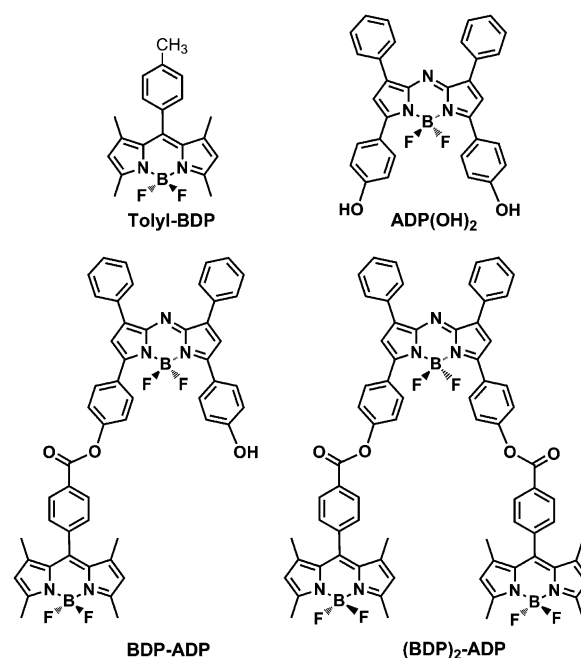
that feature ferrocene and ADP and demonstrated efficient photoinduced electron transfer from ferrocene to singlet excited ADP.<sup>[22a]</sup> By using transient absorption techniques, it was possible to spectrally characterize the one-electron-reduced product of ADP and monitor the photoinduced electron-transfer dynamics. In a parallel study, ADP was covalently linked to a known electron acceptor, fullerene, and ultrafast photoinduced electron transfer leading into the formation of a radical ion pair ( $\text{ADP}^{+\cdot} - \text{C}_{60}^{-\cdot}$ ) was successfully demonstrated.<sup>[22b]</sup>

Herein, we report on the application of both ADP and BDP in excitation-transfer and electron-transfer model compounds. For this purpose we have covalently linked one or two units of BDP to ADP and formed molecular dyad and triad systems, as shown in Scheme 1. Although structurally similar, the BDP and ADP macrocycles differ substantially in their optical absorption and emission properties in such a fashion that energy transfer from singlet excited BDP to ADP (a near-IR emitter) is achievable. This has been demonstrated herein by employing both steady-state and time-resolved studies at different time scales. In the examined BDP-ADP and  $(\text{BDP})_2\text{-ADP}$  molecules, the BDP acts both as antenna and electron-donor unit, whereas the ADP acts as a promising energy and electron acceptor. Therefore, we have successfully demonstrated the ability of singlet excited BDP to be an energy donor and an electron donor within a molecular dyad or triad. This is in contrast to the previous studies in which  $^1\text{BDP}^*$  was primarily deactivated by either one of the two photochemical processes but not both.<sup>[10–18]</sup>

## Results and Discussion

### Syntheses of the BDP-ADP dyad and $(\text{BDP})_2\text{-ADP}$ triad:

The synthesis of the donor-acceptor systems involved a multi-step approach, as shown in Scheme 2; the details are given in the Experimental Section. Briefly, the  $\text{BF}_2$ -chelated [5-(4-hydroxyphenyl)-3-phenyl-1*H*-pyrrol-2-yl]-[5-(4-hydroxyphenyl)-3-phenylpyrrol-2-ylidene]-amine was synthesized according our earlier reported procedure.<sup>[22a]</sup> Next, this compound was treated with 4-formylcarboxylic acid in the presence of EDCI to introduce one or two formyl groups on the ADP periphery. The formyl groups were reacted with 2,4-dimethylpyrrole to generate one or two dipyrromethane entities. Finally, the dipyrromethane entities were treated with  $\text{BF}_3\text{OEt}_2$  to

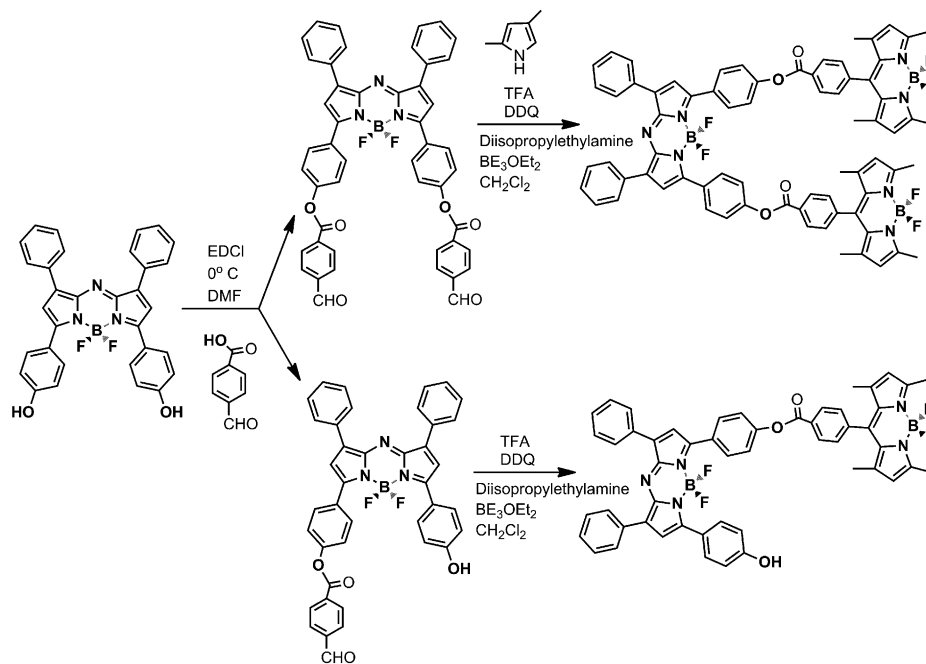


Scheme 1. Structures of the newly synthesized BDP-ADP dyad and  $(\text{BDP})_2\text{-ADP}$  triad and the  $\text{ADP}(\text{OH})_2$  and tolyl-BDP control compounds.

convert them to BDP entities. The structural integrity of the newly synthesized compounds was established from  $^1\text{H}$  NMR spectroscopy, mass spectrometry (see Figure S1, Supporting Information), and optical techniques.

### Steady-state absorption and fluorescence measurements:

The optical absorption spectra of the dyad and the triad along with the control compounds, that is, BDP and



Scheme 2. Synthetic procedure adapted for the BDP-ADP dyad and  $(\text{BDP})_2\text{-ADP}$  triad.

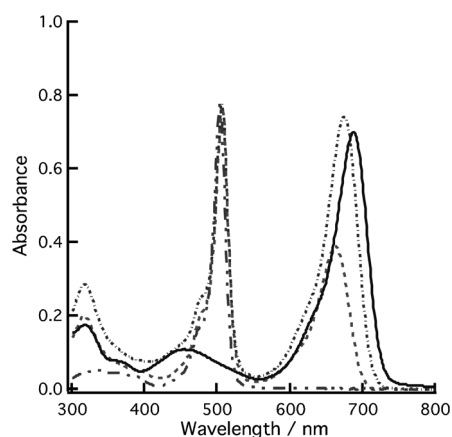


Figure 1. Normalized absorption spectra of tolyl-BDP (---),  $\text{ADP(OH)}_2$  (—), BDP-ADP (.....), and  $(\text{BDP})_2\text{-ADP}$  (-----) in toluene. The spectra of tolyl-BDP, BDP-ADP, and  $(\text{BDP})_2\text{-ADP}$  were normalized at  $\lambda = 505$  nm.

$\text{ADP(OH)}_2$ , are shown in Figure 1 in toluene and Figure S2 in the Supporting Information in benzonitrile. BDP exhibits a visible band at  $\lambda = 503$  nm, whereas for  $\text{ADP(OH)}_2$  this band is located at  $\lambda = 670$  nm, along with a less intense band at  $\lambda = 462$  nm. When pristine ADP with no peripheral OH groups is used, this band is found to be located at  $\lambda = 658$  nm. The 12 nm red shift in the spectrum of  $\text{ADP(OH)}_2$  could be ascribed to a bathochromic effect caused by the OH groups. For the BDP-ADP dyad, BDP and ADP bands are located at  $\lambda = 505$  and 676 nm, with similar peak characteristics (molar extinction coefficient ( $\epsilon$ ) and broadness). Interestingly, for the  $(\text{BDP})_2\text{-ADP}$  triad, the absorption bands are located at  $\lambda = 507$  and 665 nm, and the peak intensity of the  $\lambda = 665$  nm band corresponding to ADP is almost half of that of the BDP band at  $\lambda = 507$  nm.

Figure 2 shows the fluorescence emission spectra of the investigated compounds in toluene when excited at  $\lambda = 505$  nm, which corresponds to the absorption maxima of the BDP entity. Pristine BDP revealed a strong emission located at  $\lambda = 517$  nm ( $\Phi_f = 0.89$  for  $^1\text{BDP}^*$  and  $\Phi_f = 0.12$  for  $^1\text{ADP}^*$ ). However, in the dyad and triad this band was quantitatively quenched with the appearance of a new weak band at  $\lambda = 674$  nm for the dyad and  $\lambda = 663$  nm for the triad, respectively. The intensity of the formed  $\text{BDP}^1\text{ADP}^*$  was found to be almost the same as that obtained by the direct excitation of BDP-ADP at  $\lambda = 680$  nm in toluene, which selectively excited the ADP entity (Figure S3, Supporting Information). Further, excitation spectra for both the dyad and triad were recorded by fixing the emission monochromator to the ADP emission peak maxima. The excitation spectrum revealed the absorption band of not only ADP at  $\lambda = 671$  nm but also BDP at  $\lambda = 506$  nm, which provides direct proof for singlet–singlet energy transfer (Figure S4, Supporting Information). These results show energy transfer from the singlet-excited BDP to the covalently linked ADP in both the dyad and the triad.<sup>[23]</sup> The ratio of peak intensities was found to be 0.44, which suggests an effi-

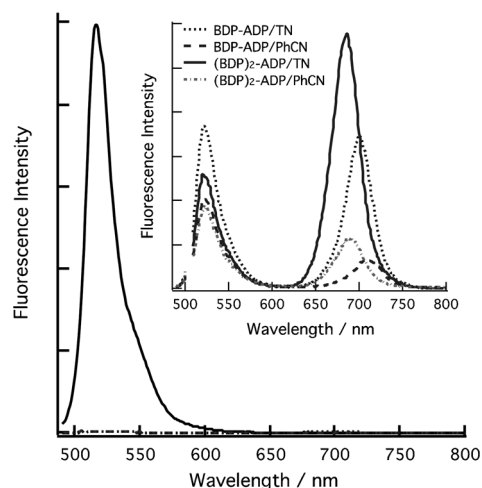


Figure 2. Fluorescence spectra of tolyl-BDP (—) and BDP-ADP dyad in toluene (.....) and benzonitrile (-----). Inset: Fluorescence spectra of the BDP-ADP dyad and  $(\text{BDP})_2\text{-ADP}$  triad in toluene (TN) and benzonitrile (PhCN) to demonstrate quenched emission of ADP in benzonitrile compared with that in toluene. The spectra were recorded at the same optical density at  $\lambda = 505$  nm;  $\lambda_{\text{ex}} = 505$  nm.

cient excitation transfer from the singlet BDP to ADP. By changing the solvent from toluene to benzonitrile, similar energy transfer from the singlet BDP to the attached ADP was clearly observed. The only difference is the considerably higher quenching of the singlet-excited states of  $\text{BDP}^1\text{ADP}^*$  and  $(\text{BDP})_2^1\text{ADP}^*$  compared to that in toluene (Figure S4, Supporting Information). These results in polar benzonitrile suggest that the  $^1\text{ADP}^*$  of the dyad and triad, formed by excitation transfer from the singlet-excited state of BDP, is further quenched by electron transfer from the attached BDP.

**Electrochemistry and energy levels:** To establish the energy levels, electrochemical studies by using differential pulse voltammetry (DPV) were performed. Figure 3 shows the DPV of the dyad and triad along with the reference compounds in *o*-dichlorobenzene (*o*-DCB), 0.10 M ( $n\text{Bu}_4\text{N})\text{ClO}_4$ . The one-electron reduction of  $\text{ADP(OH)}_2$  was located at  $-0.99$  V, whereas the one-electron reduction for tolyl-BDP is located at  $-1.75$  V vs.  $\text{Fc}/\text{Fc}^+$ . The first one-electron reduction of the BDP-ADP dyad located at  $-0.93$  V can be ascribed to the reduction of the ADP moiety, which is anodically shifted by 50 to 60 mV compared with  $\text{ADP(OH)}_2$ . The second one-electron reduction at  $-1.64$  V can be ascribed to the reduction of the BDP entity, which is found to be anodically shifted by about 106 mV compared with tolyl-BDP. Similar shifts in the reduction potentials were observed for  $(\text{BDP})_2\text{-ADP}$  triad, with the first one-electron reduction being at  $-0.85$  V and the second one-electron reduction at  $-1.65$  V, which can be attributed to reduction of the ADP and BDP entities, respectively. The one-electron oxidation potential of the tolyl-BDP is located at 0.73 V, whereas the one-electron oxidation potential corresponding to the BDP entity in  $(\text{BDP})_2\text{-ADP}$  and BDP-ADP are located at

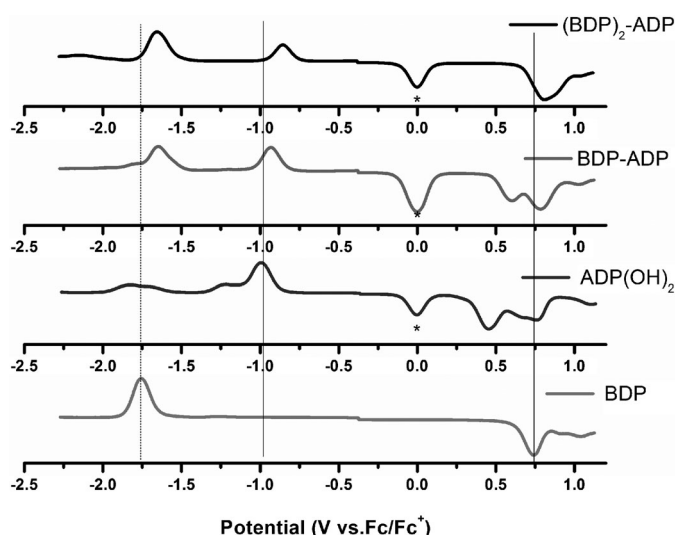


Figure 3. Differential pulse voltammograms of the indicated compounds in *o*-dichlorobenzene, 0.1 M (*n*Bu<sub>4</sub>N)ClO<sub>4</sub>. Scan rate = 5 mV s<sup>-1</sup>, pulse width = 0.25 s, pulse height = 0.025 V. The asterisk indicates the oxidation process of ferrocene used as an internal standard.

0.78 and 0.81 V versus Fc/Fc<sup>+</sup>, respectively. These anodic shifts of approximately 50 to 80 mV can be attributed to the chemical functionalization of the BDP entity. Also, in the case of the triad the current for the BDP oxidation was twice as large as that of the current of the ADP reduction. In the case of compounds with OH substituents, an additional peak near 0.7 V was observed which could be ascribed to the oxidation of phenolate substituents.

The thermodynamic driving forces for the charge-recombination ( $-\Delta G_{CR}$ ) and charge-separation ( $-\Delta G_{CS}$ ) processes were calculated by using Equations (1) and (2):<sup>[24]</sup>

$$-\Delta G_{CR} = E_{1/2}(\text{BDP}^{+/}/\text{BDP}) - E_{1/2}(\text{ADP}/\text{ADP}^{-}) + \Delta G_s \quad (1)$$

$$-\Delta G_{CS} = \Delta E_{0-0} - (-\Delta G_{CR}) \quad (2)$$

in which  $E_{1/2}(\text{BDP}^{+/}/\text{BDP})$  is the first oxidation potential of BDP,  $E_{1/2}(\text{ADP}/\text{ADP}^{-})$  is the first reduction potential of ADP,  $\Delta E_{0-0}$  is the energy of the 0–0 transition energy gap between the lowest excited state and the ground state of BDP and ADP, and  $\Delta G_s$  refers to the static Coulombic energy, calculated by using the dielectric continuum model<sup>[24]</sup> according to Equation (3):

$$\Delta G_s = -e^2/4\pi\epsilon_0[(1/(2R_+) + 1/(2R_-)) - (1/R_{CC})/\epsilon_s] - ((1/(2R_+) + 1/(2R_-))/\epsilon_R) \quad (3)$$

The symbols  $\epsilon_0$ ,  $\epsilon_s$ , and  $\epsilon_R$  represent vacuum permittivity and the dielectric constants of solvent used for photochemical and electrochemical studies, respectively.  $R_{CC}$  is the center-to-center distance between BDP and ADP entities. The  $\Delta G_{CR}$  values are summarized in Table 1. Together with

Table 1. Electrochemical redox potentials (V vs. Fc/Fc<sup>+</sup>) and driving forces of charge recombination ( $\Delta G_{CR}$ ) and charge separation ( $\Delta G_{CS}$ ) for the (BDP)<sub>n</sub>-ADP dyad ( $n=1$ ) and triad ( $n=2$ ) via <sup>1</sup>BDP\* and <sup>1</sup>ADP\* in benzonitrile and toluene.

	BDP <sup>0/+</sup> [V]	ADP <sup>0/-</sup> [V]	$\Delta G_{CR}$ <sup>[a]</sup> [eV]	$\Delta G_{CS}$ <sup>[a]</sup> [eV]	$\Delta G_{CR}$ <sup>[b]</sup> [eV]	$\Delta G_{CS}$ <sup>[b]</sup> [eV]
tolyl-BDP	0.74	–	–	–	–	–
ADP(OH) <sub>2</sub>	–	–0.99	–	–	–	–
(BDP) <sub>2</sub> <sup>-</sup>	0.78	–0.93	–1.42	–0.98 <sup>[c]</sup>	–1.88	–0.52 <sup>[c]</sup>
ADP	–	–	–	–0.43 <sup>[d]</sup>	–	– <sup>[d]</sup>
(BDP) <sub>1</sub> <sup>-</sup>	0.81	–0.85	–1.47	–0.93 <sup>[c]</sup>	–1.93	–0.47 <sup>[c]</sup>
ADP	–	–	–	–0.38 <sup>[d]</sup>	–	– <sup>[d]</sup>

[a] In benzonitrile. [b] In toluene. [c] Via <sup>1</sup>BDP\*. [d] Via <sup>1</sup>ADP\*.

the energy of <sup>1</sup>BDP\* (2.40 eV) and <sup>1</sup>ADP\* (1.85 eV), the driving forces for the charge-separation processes ( $-\Delta G_{CS}$ ) were calculated as listed in Table 1. The negative  $\Delta G_{CS}$  values of BDP-ADP and (BDP)<sub>2</sub>-ADP in benzonitrile give the charge separation from BDP to the singlet excited ADP in benzonitrile. The values of  $\Delta G_{CS}$  and  $\Delta G_{CR}$  suggest that in the event of electron transfer from BDP to <sup>1</sup>ADP\* the charge separation is in the Marcus normal region, whereas the charge recombination in BDP<sup>+</sup>-ADP<sup>-</sup> lies in the Marcus inverted region.<sup>[25]</sup>

**B3LYP/3-21G(\*) geometry optimization studies:** Figure 4a and b show the B3LYP/3-21G(\*)-optimized structures of the dyad and triad, respectively.<sup>[26,27]</sup> The structures are fully op-

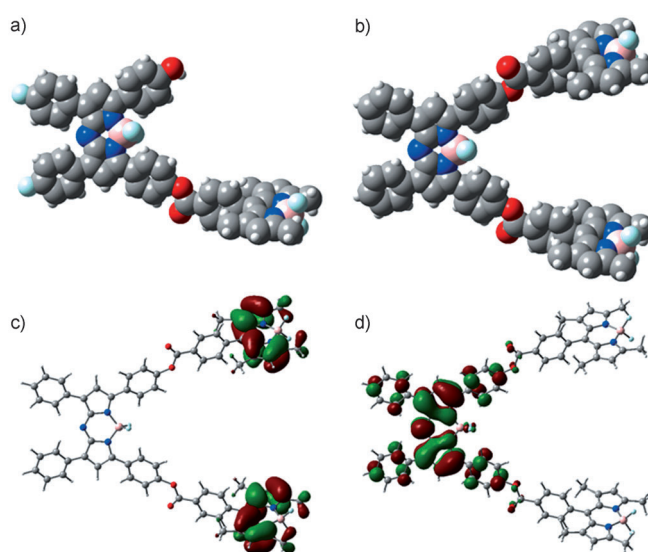


Figure 4. B3LYP/3-21G(\*) optimized structures of a) BDP-ADP and b) (BDP)<sub>2</sub>-ADP. The frontier HOMO and LUMO of the (BDP)<sub>2</sub>-ADP triad are shown in c) and d), respectively.

timized on a Born–Oppenheimer potential energy surface. In the optimized structure, both the ADP and BDP macrocycles are found to be flat, whereas the peripheral aromatic rings of ADP are slightly tilted. The boron–boron separation in the BDP-ADP macrocycles is found to be 15.6 Å, whereas the distance from the closest carbon of BDP to the closet

carbon of ADP (edge-to-edge distance) is about 12.1 Å. The two macrocycles were spatially disposed with a dihedral angle of 54.7°.

Interestingly, for the (BDP)<sub>2</sub>-ADP triad, the two coplanarly positioned BDP entities linked to ADP formed a molecular-clip-type structure similar to the structure of the (Fc)<sub>2</sub>-ADP triad reported earlier.<sup>[22a]</sup> The two BDP macrocycles are separated by a distance of 15.8 Å. The B–B separation and edge-to-edge distance are not significantly different from that of dyad. The dihedral angles between the ADP and BDP macrocycles are found to be 55.8 and 64.0° for the two BDP entities, respectively. The frontier highest occupied molecular orbital (HOMO) for both the dyad and triad are found to be on the BDP entity, while the lowest unoccupied molecular orbital (LUMO) is found to be on the ADP entity. The location of the HOMO and LUMO are in agreement with the electrochemical results, which predicted the BDP entity to be an electron donor and the ADP entity to be an electron acceptor.

**Excited energy transfer mechanism:** The observed excitation transfer between singlet-excited BDP as a donor and ADP as an acceptor could be explained either by Dexter's exchange mechanism<sup>[28]</sup> or Förster's dipole–dipole mechanism.<sup>[29]</sup> The former mechanism involves a double-electron exchange involving one electron from the LUMO of the excited donor to the empty LUMO of the acceptor with a simultaneous transfer of another electron from the HOMO of the acceptor to the half-filled HOMO of the donor. The rate constant is given by Equation (4):

$$k_D = 4\pi^2 H^2 J_D / h \quad (4)$$

in which  $h$  is Planck's constant,  $H$  is the electronic exchange parameter, and  $J_D$  is the Dexter spectral overlap integral.<sup>[28]</sup> The frontier orbitals from the DFT studies (Figure 4) in conjunction with the spectroscopic studies reveal that such electronic interactions are almost non-existent. Therefore, the results of the present study have been analyzed according to Förster's mechanism.

According to Förster mechanism, the rate of excitation energy transfer,  $k_{\text{Förster}}$ , is given by Equation (5):<sup>[29]</sup>

$$k_{\text{Förster}} = [8.8 \times 10^{-25} \kappa^2 \Phi_D J_{\text{Förster}}] / [\eta^4 \tau_D R^6] \quad (5)$$

in which  $\eta$  is the solvent refractive index,  $\Phi_D$  and  $\tau_D$  are the fluorescence quantum yield (0.6) and the fluorescence lifetime (1.6 ns) of the isolated donor,  $J_{\text{Förster}}$  is the Förster's overlap integral representing the emission of the donor and absorption of the acceptor,  $R$  is the donor–acceptor center-to-center distance (15.6 Å). In Equation (5),  $\kappa^2$  is the orientation factor and for flexible systems of the type discussed here, a value of  $\kappa^2 = 2/3$  is generally used.<sup>[23]</sup> The  $J_{\text{Förster}}$  spectral overlap integral representing the emission of the donor and absorption of the acceptor is given by Equation (6):

$$J_{\text{Förster}} = \int F_D(\lambda) \epsilon_A(\lambda) \lambda^4 d\lambda \quad (6)$$

in which  $F_D(\lambda)$  is the fluorescence intensity of the donor with total intensity normalized to unity,  $\epsilon_A(\lambda)$  is the molar extinction coefficient of the acceptor expressed in units of  $\text{M}^{-1} \text{cm}^{-1}$  and  $\lambda$  in nanometers. Analysis of the data according to Equation (6) gave a  $J$  value of  $9.1 \times 10^{-13} \text{M}^{-1} \text{cm}^3$  for the BDP-ADP system.

The  $k_{\text{Förster}}$  value estimated by using the parameters described in Equation (5) is found to be of the order of 4 to  $8 \times 10^{10} \text{s}^{-1}$ , depending upon solvent conditions, which reveals fast excitation transfer. As explained below, the rate of energy transfer measured by using the transient absorption technique agrees well with the theoretical predictions.

**Photodynamics studies:** Femtosecond transient absorption spectroscopy was used to obtain further insight into the excited state interactions in BDP-ADP dyad and (BDP)<sub>2</sub>-ADP triad to corroborate the proposed energy-transfer and electron-transfer processes. Toward this end, the BDP-ADP dyad and (BDP)<sub>2</sub>-ADP triad were probed with excitation at  $\lambda = 490 \text{ nm}$  to selectively excite the BDP fluorophore. The femtosecond transient absorption spectra of tolyl-BDP in toluene (Figure 5) revealed the instantaneous formation of

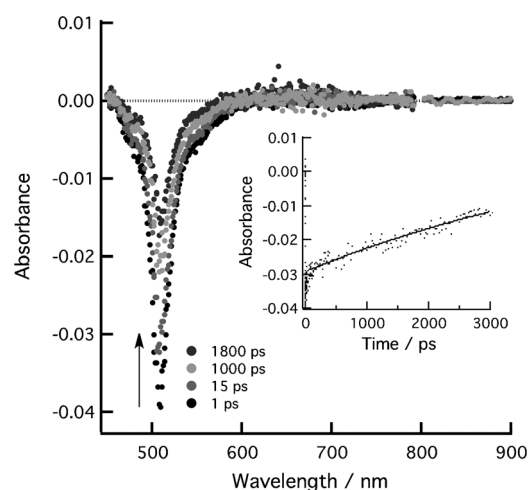


Figure 5. Differential absorption spectra obtained upon femtosecond flash photolysis ( $\lambda = 480 \text{ nm}$ ) of tolyl-BDP in toluene with several time delays between 1 and 1800 ps at room temperature. Inset: Decay profile of the singlet BDP at  $\lambda = 508 \text{ nm}$ , monitoring the intersystem crossing dynamics.

BDP singlet-excited-state features. Here, the transient absorption spectra are dominated by pronounced bleaching between  $\lambda = 450$  and  $600 \text{ nm}$ , which is due to depletion of the singlet ground state. BDP singlet-excited-state features are long lived (i.e., 4.2 ns). A slow intersystem crossing to the corresponding triplet state of BDP is implicit.

The spectral features in the visible region, which are seen immediately (i.e., 1 ps) upon excitation of BDP-ADP dyad in toluene (Figure 6), are almost the same as those recorded

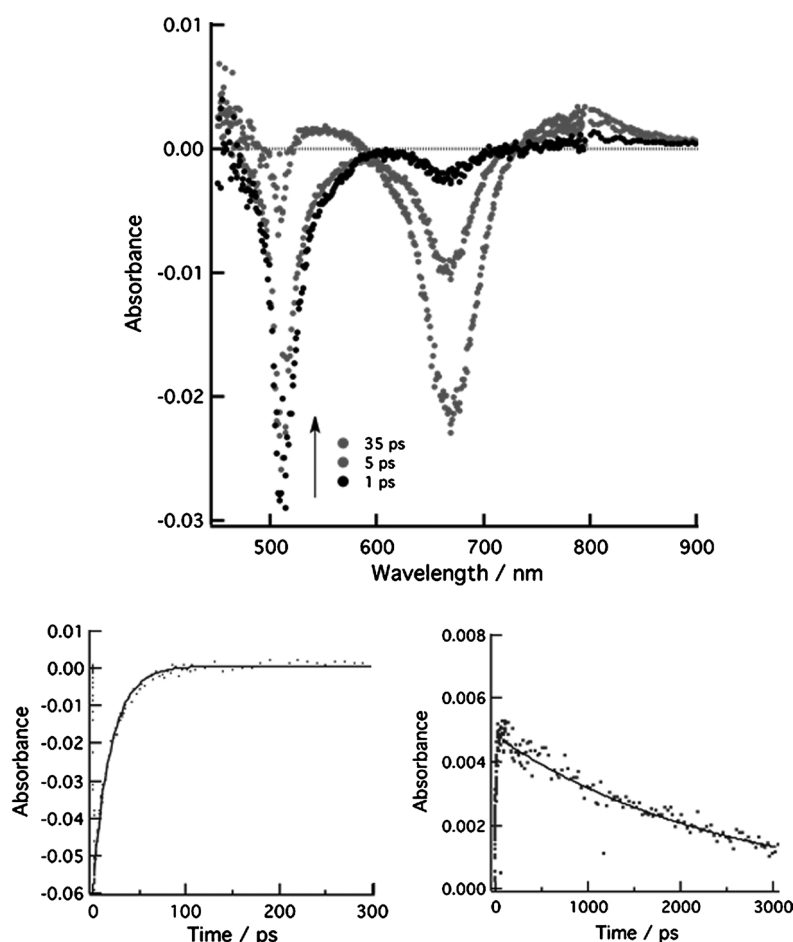


Figure 6. Top: Differential absorption spectra obtained upon femtosecond flash photolysis ( $\lambda_{\text{ex}}=490$  nm) of BDP-ADP in toluene at 1, 5, and 35 ps. Bottom: Time-absorption profiles of the singlet states of BDP (left,  $\lambda=508$  nm) and ADP (right,  $\lambda=820$  nm).

for the BDP singlet-excited state ( $^1\text{BDP}^*$ ). The absorption of the singlet BDP at  $\lambda=508$  nm is greatly diminished in intensity over time, with concomitant increase of the ADP emission at  $\lambda=671$  and  $820$  nm, which provides direct evidence of excitation transfer between the photoexcited BDP unit and the singlet ground state of ADP (see Figure S3 in the Supporting Information for femtosecond transient spectra of  $\text{ADP}(\text{OH})_2$ ). The kinetics of BDP to ADP energy transfer was determined by exponential fitting of the rise profile of the formed  $^1\text{ADP}^*$  at  $820$  nm ( $k_{\text{ENT}}=1.1 \times 10^{11} \text{ s}^{-1}$ ). The decay rate of the formed  $^1\text{ADP}^*$  was found to be  $5.7 \times 10^8 \text{ s}^{-1}$ , which is close to the decay of the singlet ADP reference compound, indicating that the  $^1\text{ADP}^*$  is not quenched by the attached BDP in toluene.

By changing the solvent from toluene to benzonitrile, similar spectral features of the BDP-ADP dyad were observed (Figure 7). From the rise profile of the formed  $^1\text{ADP}^*$ , the singlet BDP to ADP energy transfer in polar benzonitrile determined as  $1.2 \times 10^{11} \text{ s}^{-1}$ . The finding that the  $k_{\text{ENT}}$  value in benzonitrile is nearly as same as the value in toluene indicates that the energy transfer from  $^1\text{BDP}^*$  to ADP is insensitive to the solvent polarity. On the other hand,  $^1\text{ADP}^*$  de-

cayed with a rate constant of  $1.9 \times 10^9 \text{ s}^{-1}$ , which is much faster than that observed in toluene. This observation indicates occurrence of electron transfer from BDP to  $^1\text{ADP}^*$  in benzonitrile with a rate constant of  $1.40 \times 10^9 \text{ s}^{-1}$ ,<sup>[30]</sup> as predicated from the earlier steady-state emission measurements and the calculated negative  $\Delta G_{\text{CS}}$  value in benzonitrile. It should be noted that the anticipated absorption band of the ADP radical anion (Figure S6, Supporting Information) was hidden under the strong bleaching of the  $^1\text{ADP}^*$ .

The spectral features of the  $(\text{BDP})_2$ -ADP triad in toluene and benzonitrile (see Figure S7 and S8, Supporting Information) were found to be similar to those recorded for the BDP-ADP dyad. The  $k_{\text{ENT}}$  from  $^1\text{BDP}^*$  to ADP was determined to be  $1.2 \times 10^{11} \text{ s}^{-1}$ . In benzonitrile, the  $^1\text{ADP}^*$  of the  $(\text{BDP})_2$ -ADP triad decayed with a rate constant of  $6.9 \times 10^9 \text{ s}^{-1}$ , which corresponds to the  $k_{\text{CS}}$ . The faster  $k_{\text{CS}}$  of the triad with a relatively higher  $\Delta G_{\text{CS}}$  ( $-0.43$  eV) than the dyad ( $\Delta G_{\text{CS}} = -0.38$  eV) can be understood if

charge separation is occurring in the Marcus normal region.<sup>[25]</sup>

Further nanosecond transient absorption spectra were recorded to check whether the charge-separated state ( $\text{BDP}^{++}-\text{ADP}^{--}$ ) returns to the ground state via the triplet decay path. Upon excitation with  $\lambda=490$  nm laser light, the transient spectra of tolyl-BDP exhibited an extremely weak absorption in the  $\lambda=400$  to  $450$  nm range, which corresponds to triplet BDP with a lifetime of  $71 \mu\text{s}$  (Figure S9 in the Supporting Information). By exciting the  $\text{ADP}(\text{OH})_2$  control at  $\lambda=490$  nm, a weak absorption of the triplet ADP was observed in the  $\lambda=400$  to  $550$  nm range, with a maximum at  $\lambda=440$  nm (Figure S10 in the Supporting Information). The decay rate of triplet ADP was found to be  $5.7 \times 10^3 \text{ s}^{-1}$ , from which a lifetime of  $175 \mu\text{s}$  was deduced. Because the energy levels of the charge-separated states of the dyad and triad are found to be higher than that of the low-lying triplet state of ADP, the charge recombination of the radical-ion pairs can be expected to populate the triplet ADP and the ground state. The finding that the transient spectrum of  $(\text{BDP})_2$ -ADP in benzonitrile exhibited rather weak signals in the  $\lambda=400$  to  $500$  nm range, which corresponds to the for-

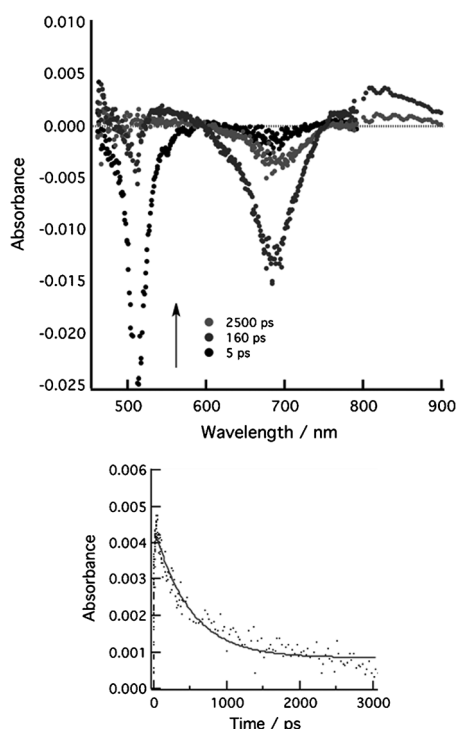


Figure 7. Top: Differential absorption spectra obtained upon femtosecond flash photolysis ( $\lambda_{\text{ex}} = 490$  nm) of BDP-ADP in benzonitrile at 5, 160, and 2500 ps. Bottom: Time-absorption profile of the singlet state of ADP at  $\lambda = 820$  nm, monitoring the energy-transfer and electron-transfer dynamics.

mation of triplet ADP (Figure S11, Supporting Information), suggests that the transient species of both dyad and triad decayed mainly to populate the ground state.

Figure 8 summarizes the photochemical events in the form of an energy-level diagram for the investigated dyad; a similar diagram can be envisioned for the triad as well. Selective excitation of the BDP entity of the dyad populates the singlet-excited state of BDP, which transfers its energy

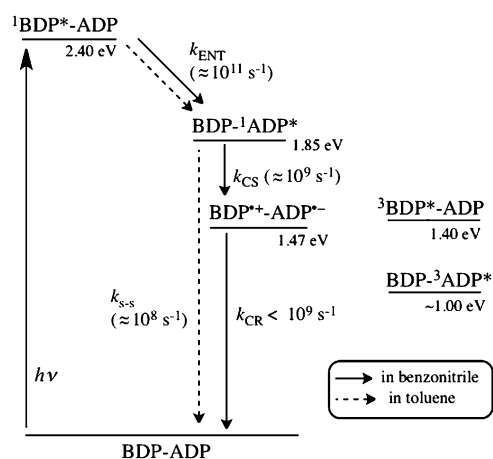


Figure 8. Energy-level diagram depicting photoinduced energy-transfer and electron-transfer processes in the BDP-ADP dyad in benzonitrile and toluene.

to the attached ADP. In toluene, the formed  $^1\text{ADP}^*$  decayed to its ground state without evidence of additional subsequent energy-transfer and/or electron-transfer reactions. However, an electron transfer from BDP to  $^1\text{ADP}^*$  in benzonitrile was clearly observed to give  $(\text{BDP}^{+\cdot}-\text{ADP}^{\cdot-})$  in both dyad and triad. It is worth noting that deactivation of the electron-transfer product,  $\text{BDP}^{+\cdot}-\text{ADP}^{\cdot-}$  leads to the ground state without the intermediate formation of either  $^3\text{BDP}^*$  or  $^3\text{ADP}^*$ , as indicated by the photochemical measurements.

## Conclusion

The synthesis and characterization of a new type of dyad and triad featuring  $\text{BF}_2$ -chelated dipyrromethane covalently linked to its structural analog,  $\text{BF}_2$ -chelated tetraarylazadipyrromethane, have been accomplished. The structural integrity of the newly synthesized dyad and triad has been established by spectroscopic, electrochemical, and computational methods. DFT calculations revealed a molecular-clip-type structure for the triad, in which the two coplanar BDP entities are separated by about 16 Å. The redox states were examined by using voltammetry studies, and the free-energy calculations suggested the possibility of charge separation via the singlet-excited states of BDP and ADP entities. However, selective excitation of the BDP entity in the dyad and triad revealed quantitative quenching of the BDP fluorescence with simultaneous emission from the ADP entity in the near-IR region in both polar and nonpolar solvents. The energy-transfer and electron-transfer products were characterized by the femtosecond laser flash photolysis studies. The kinetics of energy transfer, measured by monitoring either the decay of BDP emission or the rise of the ADP emission, revealed fast energy transfer ( $\approx 10^{11} \text{ s}^{-1}$ ) in these molecular systems in both polar and nonpolar solvents, which agrees well with the theoretical estimations. In contrast to the results obtained in toluene, further photochemical events from BDP to  $^1\text{ADP}^*$  that lead to electron transfer are observed in polar benzonitrile. The kinetics of this process were found to be relatively fast. The present study successfully demonstrates utilization of a near-IR emitting sensitizer,  $\text{BF}_2$ -chelated tetraarylazadipyrromethane, as a suitable candidate to build new types of donor-acceptor dyads for excitation-transfer and electron-transfer studies.

## Experimental Section

**Chemicals:** All the reagents were from Aldrich Chemicals (Milwaukee, WI), whereas the bulk solvents used in the syntheses were from Fischer Chemicals. Tetra-*n*-butylammonium perchlorate,  $(n\text{Bu}_4\text{N})\text{ClO}_4$  used in electrochemical studies were from Fluka Chemicals. The initial synthesis of ADP macrocycle was performed according to the procedure reported by O'Shea and co-workers<sup>[20]</sup> with modifications.

The synthetic details of  $\text{BF}_2$ -chelated [5-(4-hydroxyphenyl)-3-phenyl-1*H*-pyrrol-2-yl]-[5-(4-hydroxyphenyl)-3-phenylpyrrol-2-ylidene]amine are provided elsewhere.<sup>[23]</sup>

**Synthesis of ADP-(ALDEHYDE)<sub>2</sub> and ADP-(ALDEHYDE)<sub>1</sub>:** 4-Carboxybenzaldehyde (200 mg, 1.3 mmol) was dissolved in DMF (20 cm<sup>3</sup>), to which EDCI (255 mg, 1.3 mmol) was added at 0 °C under N<sub>2</sub>, followed by the addition of BF<sub>2</sub>-chelated [5-(4-hydroxyphenyl)-3-phenyl-1*H*-pyrrol-2-yl]-[5-(4-hydroxyphenyl)-3-phenylpyrrol-2-ylidene]amine (234.9 mg, 0.4 mmol; see Scheme 2 for structures of the abbreviated compounds), after which the mixture was stirred for 24 h. Then the solvent was removed under reduced pressure and the residue was dissolved in CH<sub>2</sub>Cl<sub>2</sub> and washed with water. Then the organic layer was separated and dried over Na<sub>2</sub>SO<sub>4</sub>, then the solvent was evaporated. The residue was purified by column chromatography on silica gel with CH<sub>2</sub>Cl<sub>2</sub>/hexanes (1:1) to give ADP-(ALDEHYDE)<sub>2</sub> (yield 80 mg, 22%), and with CH<sub>2</sub>Cl<sub>2</sub> to give ADP-(ALDEHYDE)<sub>1</sub> (yield 50 mg, 17%).

**Data for ADP-(ALDEHYDE)<sub>2</sub>:** <sup>1</sup>H NMR (400 MHz, CDCl<sub>3</sub>): δ = 10.16 (s, 2H), 8.38 (d, *J* = 8.14 Hz, 4H), 8.17 (d, *J* = 8.98 Hz, 4H), 8.12–8.02 (m, 8H), 7.52–7.45 (m, 6H), 7.41 (d, *J* = 8.96 Hz, 4H), 7.08 ppm (s, 2H)

**Data for ADP-(ALDEHYDE)<sub>1</sub>:** <sup>1</sup>H NMR (400 MHz, CDCl<sub>3</sub>): δ = 10.17 (s, 1H), 8.39 (d, *J* = 8.34 Hz, 2H), 8.14 (d, *J* = 9.04 Hz, 2H), 8.11–8.03 (m, 10H), 7.52–7.41 (m, 8H), 7.38 (d, *J* = 8.95 Hz, 2H), 7.11 (s, 1H), 7.01 (s, 1H), 6.96 ppm (d, *J* = 8.88 Hz, 2H).

**Synthesis of (BDP)<sub>2</sub>-ADP:** Compound ADP-(ALDEHYDE)<sub>2</sub> (63 mg, 8 × 10<sup>-2</sup> mmol) and 2,4-dimethyl pyrrole (3.3 × 10<sup>-2</sup> cm<sup>3</sup>, 0.32 mmol) were dissolved in absolute methylene chloride (50 cm<sup>3</sup>) under N<sub>2</sub>. One drop of trifluoroacetic acid was added to the reaction mixture, which was stirred for 3 h. Then a solution of DDQ (36 mg, 0.16 mmol) in methylene chloride was added and the mixture was stirred for 1 h followed by the addition of diisopropylethylamine (0.12 cm<sup>3</sup>, 0.68 mmol) and borontrifluoride diethyletherate (0.12 cm<sup>3</sup>, 0.97 mmol). The reaction mixture was stirred for a further 1 h, after which it was washed with water. The organic layer was dried over anhydrous Na<sub>2</sub>SO<sub>4</sub> and the solvent was evaporated. The residue was purified by column chromatography on silica gel with CH<sub>2</sub>Cl<sub>2</sub>/hexanes (1:1) to give (BDP)<sub>2</sub>-ADP (Yield: 10 mg, 10%). <sup>1</sup>H NMR (400 MHz, CDCl<sub>3</sub>): δ = 8.35 (d, *J* = 8.28 Hz, 4H), 8.18 (d, *J* = 8.82 Hz, 4H), 8.09 (d, *J* = 9.59 Hz, 4H), 7.56–7.4 (m, 14H), 7.08 (s, 2H), 6.02 (s, 2H), 2.58 (s, 12H), 1.42 ppm (s, 12H); MALDI MS: *m/z* calcd for C<sub>22</sub>H<sub>36</sub>N<sub>7</sub>O<sub>4</sub>B<sub>3</sub>F<sub>6</sub>: 1229.7; found: 1236.07.

**Synthesis of (BDP)<sub>1</sub>-ADP:** Compound ADP-(ALDEHYDE)<sub>1</sub> (40 mg, 6 × 10<sup>-2</sup> mmol) and 2,4-dimethyl pyrrole (1.2 × 10<sup>-2</sup> cm<sup>3</sup>, 0.12 mmol) were dissolved in (50 cm<sup>3</sup>) absolute methylene chloride under N<sub>2</sub> atmosphere. To the reaction mixture one drop of trifluoroacetic acid was added and was stirred for a period of 3 h. Then a solution of DDQ (13.7 mg, 6 × 10<sup>-2</sup> mmol) in methylene chloride was added, and the stirring was continued for 1 h followed by the addition of diisopropylethylamine (0.12 cm<sup>3</sup>, 0.68 mmol) and borontrifluoride diethyletherate (0.12 cm<sup>3</sup>, 0.97 mmol). Stirring was further continued for 1 h, after which the reaction mixture was washed with water. The organic layer was dried over anhydrous Na<sub>2</sub>SO<sub>4</sub> and the solvent was evaporated. The residue was purified by column chromatography on silica gel with CH<sub>2</sub>Cl<sub>2</sub> to give (BDP)<sub>1</sub>-ADP (yield 8 mg, 15%). <sup>1</sup>H NMR (400 MHz, CDCl<sub>3</sub>): δ = 8.35 (d, *J* = 8.38 Hz, 2H), 8.13 (d, *J* = 8.86 Hz, 2H), 8.02–8.10 (m, 8H), 7.52–7.36 (m, 8H), 7.1 (s, 1H), 7.0 (s, 1H), 6.93 (d, *J* = 8.7, 2H), 6.02 (s, 2H), 2.58 (s, 6H), 1.42 ppm (s, 6H); MALDI MS: *m/z* calcd for C<sub>22</sub>H<sub>41</sub>N<sub>5</sub>O<sub>3</sub>F<sub>4</sub>B<sub>2</sub>: 880.6; found: 884.3.

**Spectral measurements:** The UV/Vis spectral measurements were carried out with a Shimadzu Model 2550 double monochromator UV/Vis spectrophotometer. The fluorescence emission was monitored by using a Varian Eclipse spectrometer. A right-angle detection method was used. The <sup>1</sup>H NMR studies were carried out by using a Varian 400 MHz spectrometer. Tetramethylsilane (TMS) was used as an internal standard. Differential pulse voltammograms were recorded by using an EG&G PAR-STAT electrochemical analyzer equipped with a three electrode system. A platinum button electrode was used as the working electrode. A platinum wire served as the counter electrode and an Ag/AgCl electrode was used as the reference electrode. The ferrocene/ferrocenium redox couple was used as an internal standard. All the solutions were purged prior to electrochemical and spectral measurements using argon gas. Matrix-assisted laser desorption/ionization time-of-flight mass spectra (MALDI-TOF) were measured by using a Kratos Compact MALDI II (Shimadzu)

for metal complexes in PhCN with dithranol as a matrix. The computational calculations were performed by using DFT B3LYP/3-21G\* methods with the GAUSSIAN 03 software package<sup>[27]</sup> on high-speed PCs. The frontier HOMO and LUMO were generated by using GaussView software.

The studied compounds were excited by a Panther OPO pumped by Nd/YAG laser (Continuum, SLII-10, 4–6 ns fwhm) with the powers of 1.5 and 3.0 mJ pulse<sup>-1</sup>. The transient absorption measurements were performed by using a continuous xenon lamp (150 W) and an InGaAs-PIN photodiode (Hamamatsu 2949) as a probe light and a detector, respectively. The output from the photodiodes and a photomultiplier tube was recorded with a digitizing oscilloscope (Tektronix, TDS3032, 300 MHz). Femtosecond transient absorption spectroscopy experiments were conducted by using an Integra-C (Quantronix Corp.) as an ultrafast source, TOPAS (Light Conversion Ltd.) as an optical parametric amplifier, and a commercially available optical detection system (Helios, provided by Ultrafast Systems LLC). The source for the pump and probe pulses were derived from the fundamental output of the Integra-C (780 nm, 2 mJ pulse<sup>-1</sup>, and fwhm = 130 fs) at a repetition rate of 1 kHz. 75% of the fundamental output of the laser was introduced into TOPAS, which has optical frequency mixers that result in a tunable range from λ = 285 to 1660 nm, whereas the rest of the output was used for white light generation. Typically, 2500 excitation pulses were averaged for 5 s to obtain the transient spectrum at a set delay time. Kinetic traces at appropriate wavelengths were assembled from the time-resolved spectral data. All measurements were conducted at 298 K. The transient spectra were recorded using fresh solutions in each laser excitation.

## Acknowledgements

The authors are thankful to Drs. E. Maligaspe and N. K. Subbaiyan for helpful discussions. This work was supported by the National Science Foundation (grant nos. CHE-0804015 and CHE1110942 to F.D.), a Grant-in-Aid (nos. 20108010 and 21750146), and the Global COE (center of excellence) program "Global Education and Research Center for Bio-Environmental Chemistry" of Osaka University from the Ministry of Education, Culture, Sports, Science, and Technology, Japan, and KOSEF/MEST through WCU project (R31-2008-000-10010-0) from Korea.

- [1] a) D. Gust, T. A. Moore, A. L. Moore, *Acc. Chem. Res.* **2009**, *42*, 1890–1898; b) D. Gust, T. A. Moore in *The Porphyrin Handbook*, Vol. 8 (Eds.: K. M. Kadish, K. M. Smith, R. Guilard), Academic Press, San Diego, **2000**, pp. 153–190.
- [2] a) M. R. Wasielewski, *Acc. Chem. Res.* **2009**, *42*, 1910–1921; b) M. R. Wasielewski, *Chem. Rev.* **1992**, *92*, 435–461.
- [3] a) G. de La Torre, P. Vazquez, F. Agullo-Lopez, T. Torres, *Chem. Rev.* **2004**, *104*, 3723–3750; b) G. Bottari, G. de La Torre, D. M. Guldi, T. Torres, *Chem. Rev.* **2010**, *110*, 6768–6816; c) D. M. Guldi, G. M. A. Rahman, V. Sgobba, C. Ehli, *Chem. Soc. Rev.* **2006**, *35*, 471–487; d) S. Fukuzumi, D. M. Guldi in *Electron Transfer in Chemistry*, Vol. 2 (Ed.: V. Balzani), Wiley-VCH, Weinheim, **2001**, pp. 270–337; e) L. Sánchez, M. Nazario, D. M. Guldi, *Angew. Chem.* **2005**, *117*, 5508; *Angew. Chem. Int. Ed.* **2005**, *44*, 5374.
- [4] a) V. Balzani, G. Bergamini, P. Ceroni, *Coord. Chem. Rev.* **2008**, *252*, 2456–2469; b) W. M. Campbell, A. K. Burrell, D. L. Officer, K. W. Jolley, *Coord. Chem. Rev.* **2004**, *248*, 1363–1379; c) M. D. Ward, *Chem. Soc. Rev.* **1997**, *26*, 365–375; d) V. Balzani, A. Credi, M. Venturi, *ChemSusChem* **2008**, *1*, 26; e) J. L. Sessler, C. M. Lawrence, J. Jayawickramarajah, *Chem. Soc. Rev.* **2007**, *36*, 314–325.
- [5] a) F. D'Souza, O. Ito, *Coord. Chem. Rev.* **2005**, *249*, 1410–1422; b) F. D'Souza, O. Ito, *Chem. Commun.* **2009**, 4913–4928; c) M. E. El-Khouly, O. Ito, P. M. Smith, F. D'Souza, *J. Photochem. Photobiol. C* **2004**, *5*, 79–104; d) F. D'Souza, O. Ito, *Chem. Soc. Rev.* **2012**, *41*, 86–96; e) F. D'Souza, O. Ito in *Multiporphyrin Arrays: Fundamen-*

- tals and Applications* (Ed.: D. Kim), Pan Stanford, Singapore, **2012**, pp. 389–437.
- [6] a) S. Fukuzumi, *Org. Biomol. Chem.* **2003**, *1*, 609–620; b) S. Fukuzumi, *Bull. Chem. Soc. Jpn.* **2006**, *79*, 177–195; c) S. Fukuzumi, *Phys. Chem. Chem. Phys.* **2008**, *10*, 2283–2297; d) S. Fukuzumi, T. Kojima, *J. Mater. Chem.* **2008**, *18*, 1427–1439; e) S. Fukuzumi, T. Honda, K. Ohkubo, T. Kojima, *Dalton Trans.* **2009**, 3880–3889.
- [7] a) *An Introduction to Molecular Electronics*, (Eds.: M. C. Petty, M. R. Bryce, D. Bloor), Oxford University Press, New York, **1995**; b) *Molecular Electronics: Science and Technology* (Eds.: A. Aviram, M. Ratner), New York Academy of Sciences, New York, **1998**, 852; c) *Molecular Switches* (Ed.: B. L. Feringa), Wiley-VCH, Weinheim, **2001**; d) D. Gust, T. A. Moore, A. L. Moore, *Chem. Commun.* **2006**, 1169; e) V. Balzani, A. Credi, M. Venturi in *Organic Nanostructures* (Eds.: J. L. Atwood, J. W. Steed), **2008**, 1–31; f) *Energy Harvesting Materials* (Ed.: D. L. Andrews), World Scientific, Singapore, **2005**; g) *Molecular Electronics: Commercial Insights, Chemistry, Devices, Architectures and Programming* (Ed.: J. M. Tour), World Scientific, River Edge, NJ, **2003**.
- [8] a) *The Porphyrin Handbook, Vol. 1–20* (Eds.: K. M. Kadish, K. M. Smith, R. Guilard), Academic Press, San Diego, CA, **2000**; b) *Phthalocyanine: Properties and Applications* (Eds.: C. C. Leznoff, A. B. P. Lever), Wiley-Blackwell, New York, **1993**; c) C. G. Claessens, D. González-Rodríguez, T. Torres, *Chem. Rev.* **2002**, *102*, 835.
- [9] a) A. Treibs, F. H. Kreuzer, *Justus Liebig's Ann. Chem.* **1968**, *718*, 208–223; b) *Handbook of Fluorescent Probes and Research Chemicals* (Ed.: R. P. Haugland), Molecular Probes, Eugene, OR, **1996**.
- [10] a) D. P. Kennedy, C. M. Kormos, S. Burdette, *J. Am. Chem. Soc.* **2009**, *131*, 8578–8586; b) J. Rosenthal, S. J. Lippard, *J. Am. Chem. Soc.* **2010**, *132*, 5536–5537.
- [11] a) Y. C. Lee, J. T. Hupp, *Langmuir* **2010**, *26*, 3760–3765; b) J. Godoy, G. Vives, J. M. Tour, *Org. Lett.* **2010**, *12*, 1464–1467.
- [12] A. Nierth, A. Y. Kobitski, G. U. Nienhaus, A. Jäschke, *J. Am. Chem. Soc.* **2010**, *132*, 2646–2654.
- [13] J. Karolin, L. B.-A. Johansson, L. Strandberg, T. Ny, *J. Am. Chem. Soc.* **1994**, *116*, 7801–7806.
- [14] a) H. Imahori, H. Norieda, H. Yamada, Y. Nishimura, I. Yamazaki, Y. Sakata, S. Fukuzumi, *J. Am. Chem. Soc.* **2001**, *123*, 100–110; b) S. Hattori, K. Ohkubo, Y. Urano, H. Sunahara, T. Nagano, Y. Wada, N. V. Tkachenko, H. Lemmetyinen, S. Fukuzumi, *J. Phys. Chem. B* **2005**, *109*, 15368–15375.
- [15] a) M. T. Whited, P. I. Djurovich, S. T. Roberts, A. C. Durrell, C. W. Schlenker, S. E. Bradforth, M. E. Thompson, *J. Am. Chem. Soc.* **2011**, *133*, 88–96; b) T. Lazarides, T. M. McCormick, K. C. Wilson, S. Lee, D. W. McCamant, R. Eisenberg, *J. Am. Chem. Soc.* **2011**, *133*, 350–364; c) T. H. Allik, R. E. Hermes, G. Sathyamoorthi, J. H. Boyer, *Proc. SPIE* **1994**, *2115*, 240–248.
- [16] a) F. D'Souza, P. M. Smith, M. E. Zandler, A. L. McCarty, M. Itou, Y. Araki, O. Ito, *J. Am. Chem. Soc.* **2004**, *126*, 7898–7907; b) C. A. Wijesinghe, M. E. El-Khouly, J. D. Blakemore, M. E. Zandler, S. Fukuzumi, F. D'Souza, *Chem. Commun.* **2010**, 46, 3301–3303; c) C. A. Wijesinghe, M. E. El-Khouly, N. K. Subbaiyan, M. Supur, M. E. Zandler, K. Ohkubo, S. Fukuzumi, F. D'Souza, *Chem. Eur. J.* **2011**, *17*, 3147–3156; d) F. D'Souza, C. A. Wijesinghe, M. E. El-Khouly, J. Hudson, M. Niemi, H. Lemmetyinen, N. V. Tkachenko, M. E. Zandler, S. Fukuzumi, *Phys. Chem. Chem. Phys.* **2011**, *13*, 18168–18178.
- [17] a) J.-Y. Liu, M. E. El-Khouly, S. Fukuzumi, D. K. P. Ng, *Chem. Asian J.* **2011**, *6*, 174–179; b) J.-Y. Liu, M. E. El-Khouly, S. Fukuzumi, D. K. P. Ng, *Chem. Eur. J.* **2011**, *17*, 1605–1613.
- [18] a) T. Lazarides, G. Charalambidis, A. Vuillamy, M. Reglier, E. Klontzas, G. Froudakis, S. Kuhri, D. M. Guldi, A. G. Coutsolelos, *Inorg. Chem.* **2011**, *50*, 8926–8936; b) F. Li, S. I. Yang, T. Ciringh, J. Seth, C. H. Martin, D. L. Singh, D. Kim, R. R. Birge, D. F. Bocian, D. Holten, J. S. Lindsey, *J. Am. Chem. Soc.* **1998**, *120*, 10001–10017.
- [19] A. Loudet, K. Burgess, *Chem. Rev.* **2007**, *107*, 4891–4932.
- [20] a) A. Gorman, J. Killoran, C. O'Shea, T. Kenna, W. M. Gallagher, D. F. O'Shea, *J. Am. Chem. Soc.* **2004**, *126*, 10619–10631; b) M. Tasior, D. F. O'Shea, *Bioconjugate Chem.* **2010**, *21*, 1130–1133.
- [21] a) A. Palma, M. Tasior, D. O. Frimannsson, T. T. Vu, R. Meallet-Re-nault, D. F. O'Shea, *Org. Lett.* **2009**, *11*, 3638–3641; b) J. Murtagh, D. O. Frimannsson, D. F. O'Shea, *Org. Lett.* **2009**, *11*, 5386–5389; c) S. O. McDonnell, M. J. Hall, L. T. Allen, A. Byrne, W. M. Gallagher, D. F. O'Shea, *J. Am. Chem. Soc.* **2005**, *127*, 16360–16361; d) K. Flavin, K. Lawrence, J. Bartelmess, M. Tasior, C. Navio, C. Bittencourt, D. F. O'Shea, D. M. Guldi, S. Giordani, *ACS Nano* **2011**, *5*, 1198–1206; e) Y. Kotaoka, Y. Shibata, H. Tamiaki, *Chem. Lett.* **2010**, *39*, 953–955.
- [22] a) A. N. Amin, M. E. El-Khouly, N. K. Subbaiyan, M. E. Zandler, M. Supur, S. Fukuzumi, F. D'Souza, *J. Phys. Chem. A* **2011**, *115*, 9810–9819; b) A. N. Amin, M. E. El-Khouly, N. K. Subbaiyan, M. E. Zandler, S. Fukuzumi, F. D'Souza, *Chem. Commun.* **2012**, *48*, 206–208; c) F. D'Souza, A. N. Amin, M. E. El-Khouly, N. K. Subbaiyan, M. E. Zandler, S. Fukuzumi, *J. Am. Chem. Soc.* **2012**, *134*, 654–664.
- [23] *Principles of Fluorescence Spectroscopy*, 3rd ed. (Ed.: J. R. Lakowicz), Springer, Singapore, **2006**.
- [24] N. Mataga, H. Miyasaka in *Electron Transfer, Part 2: From Isolated Molecules to Biomolecules* (Eds.: J. Jortner, M. Bixon), John Wiley & Sons, New York, **1999**, pp. 431–496.
- [25] a) R. A. Marcus, *J. Chem. Phys.* **1965**, *43*, 679; b) R. A. Marcus, N. Sutin, *Biochim. Biophys. Acta* **1985**, *811*, 265; c) R. A. Marcus, *Angew. Chem.* **1993**, *105*, 1161; *Angew. Chem. Int. Ed. Engl.* **1993**, *32*, 1111; d) J. L. Goodman, J. E. Moser, B. Armitage, S. Farid, *J. Am. Chem. Soc.* **1989**, *111*, 3489.
- [26] Gaussian 03, Revision B.04, M. J. Frisch, G. W. Trucks, H. B. Schlegel, G. E. Scuseria, M. A. Robb, J. R. Cheeseman, J. A. Montgomery, Jr., T. Vreven, K. N. Kudin, J. C. Burant, J. M. Millam, S. S. Iyengar, J. Tomasi, V. Barone, B. Mennucci, M. Cossi, G. Scalmani, N. Rega, G. A. Petersson, H. Nakatsuji, M. Hada, M. Ehara, K. Toyota, R. Fukuda, J. Hasegawa, M. Ishida, T. Nakajima, Y. Honda, O. Kitao, H. Nakai, M. Klene, X. Li, J. E. Knox, H. P. Hratchian, J. B. Cross, V. Bakken, C. Adamo, J. Jaramillo, R. Gomperts, R. E. Stratmann, O. Yazyev, A. J. Austin, R. Cammi, C. Pomelli, J. W. Ochterski, P. Y. Ayala, K. Morokuma, G. A. Voth, P. Salvador, J. J. Dannenberg, V. G. Zakrzewski, S. Dapprich, A. D. Daniels, M. C. Strain, O. Farkas, D. K. Malick, A. D. Rabuck, K. Raghavachari, J. B. Foresman, J. V. Ortiz, Q. Cui, A. G. Baboul, S. Clifford, J. Cioslowski, B. B. Stefanov, G. Liu, A. Liashenko, P. Piskorz, I. Komaromi, R. L. Martin, D. J. Fox, T. Keith, M. A. Al-Laham, C. Y. Peng, A. Nanayakkara, M. Challacombe, P. M. W. Gill, B. Johnson, W. Chen, M. W. Wong, C. Gonzalez, J. A. Pople, Gaussian, Inc., Wallingford CT, **2004**.
- [27] For a general review on DFT applications of porphyrin-fullerene systems see: M. E. Zandler, F. D'Souza, *C. R. Chimie* **2006**, *9*, 960–981.
- [28] D. L. Dexter, *J. Chem. Phys.* **1953**, *21*, 836–850.
- [29] T. Förster, *Discuss. Faraday Soc.* **1959**, *27*, 7–17.
- [30] The rate constants of the electron transfer ( $k_{ET}$ ) for the dyad and the triad in benzonitrile are calculated according to  $k_{ET} = 1/\tau - k_D$ , in which  $k_{ET}$  is the rate constant of electron transfer,  $1/\tau$  is the experimentally observed decay time of the singlet excited state, and  $k_D$  is the rate constant of the decay of the singlet excited state other than electron transfer.

Received: September 30, 2011

Revised: December 8, 2011

Published online: March 13, 2012